


Thermodynamic GUP correction for black hole within quintessence matter

Riasat Ali^{1†}  Tiecheng Xia (夏铁成)^{2‡} Rimsha Babar^{1§}

¹Department of Mathematics, GC University Faisalabad Layyah Campus, Layyah-31200, Pakistan

²College of Science, Inner Mongolia University of Technol, Hohhot 010051, China

Abstract: We examine the black hole geometry in general relativity using Einstein's equations to modify the geometry in quintessence matter. In quintessence matter, we incorporate black hole geometry into the standard formula to assess the Hawking temperature. We implement the Hamilton-Jacobi semi-classical technique to examine the Hawking temperature of a four-dimensional black hole spacetime. The boson particles are tunnelled into the horizon under the action of the generalized uncertainty principle (GUP) by implementing the relativistic field equation and WKB strategy. The Hawking temperature is investigated under the influence of the GUP parameter, particle properties, and black hole geometry parameters. Entropy and emission energy corrections are also examined using the Hawking temperature.

Keywords: black hole geometry in quintessence matter, Hamilton-Jacobi semi-classical procedure, WKB strategy, thermodynamic properties

DOI: 10.1088/1674-1137/ae5049 **CSTR:** 32044.14.ChinesePhysicsC.50065109

I. INTRODUCTION

One of the most significant and vital foundational theories in modern science is Einstein's general relativity (*GR*), which suggests the existence of black holes (BHs) [1, 2]. A BH is described by *GR* as a space area where the field of gravitation is so strong that nothing, not even light particles, can exit from it. BHs were thought to absorb and expel nothing at all [3]. The concept of quantum mechanical theory significantly modified Stephen Hawking's idea. According to Hawking's idea in 1974, BHs have an appropriate temperature designated as the Hawking temperature (T_H) [4, 5]. According to Hawking's mathematical models, all BHs release thermal energy in the form of Hawking radiation. However, higher temperatures make this effect more noticeable for smaller, quantum-sized BHs, making the phenomenon of thermal emission very important in such scenarios. Interpreting quantum gravity theories requires knowledge of quantum implications within the framework of traditional general relativity. A decreased BH evaporation [6] via the Hamilton-Jacobi semi-classical ansatz, which applies the Lagrangian modified solution in WKB application, is the case of a quantum or GUP parameter [7]. To integrate the relativity theory of BH dynamics with conventional mechanics, the radiation mechanism was investigated [8]. Several approaches to the occurrence of Hawking radi-

ation have been presented in literature. This radiation has been the subject of numerous investigations on well-known BHs [9–21]. This radiation can be examined using a semi-classical methodology that involves a particle moving across the external horizon and tunneling of the BH from internal to external [22, 23]. The tunneling strategy is based on the null geodesic [24–26] and Hamilton–Jacobi scheme [27]. These methods derive the imagined component of the classical process from an external horizon by applying the fundamentally forbidden path of a particle.

Observable matter in the galaxy's central disk is thought to dominate the galaxy's mass by Newton's law of gravitational force. However, the curves that appear in spiral galaxies indicate that velocity appears to remain flat instead of decreasing with range beyond the visual radius of the galaxy. This conclusion suggests that the galaxy is surrounded by an unseen quintessence matter. Detecting and interpreting dark matter has emerged as one of the most significant tasks in modern physics. It has grown to be one of the most significant mysteries in our universe. In the Laser Interferometer Space Antenna (LISA), to recognise low-frequency radiation, the quintessence matter should change the spacetime's structure. The dark matter and uncertainty principle affect the Hawking radiation generated in the spacetime. In theory, the existence of dark matter could affect the spacetime

Received 17 November 2025; Accepted 11 March 2026; Accepted manuscript online 12 March 2026

[†] E-mail: riasatyasir@gmail.com

[‡] E-mail: xiatic@shu.edu.cn

[§] E-mail: rimsha.babar10@gmail.com

©2026 Chinese Physical Society and the Institute of High Energy Physics of the Chinese Academy of Sciences and the Institute of Modern Physics of the Chinese Academy of Sciences and IOP Publishing Ltd. All rights, including for text and data mining, AI training, and similar technologies, are reserved.

geometry surrounding the BH, which leads to obvious changes in Hawking radiation, entropy, orbital dynamics, and BH shadows. One can investigate such variations in a realisable analytical framework by using an efficient quintessence metric. The GUP expands the conventional Heisenberg uncertainty principle to incorporate the smallest length scales suggested by many quantum gravity models and represents an important step in our understanding of quantum gravity. The modification to BH geometry and expectations of residue at the conclusion of the evaporation of the BH have been analyzed under the GUP in the uncertainty interactions, which are crucial for the determination of spacetime singularities. With implications for high-energy scenarios and the Planck scale in physics, these results provide a solid basis for exploring the combination of quantum physics and gravity. In the minor scale of quantum gravitational interactions without GUP parameter limits, confirmation by experiment is challenging. The absence of a widely utilized interpretation of the GUP parameter leads to logical uncertainty. The GUP is a powerful theoretical tool that unifies concepts across several models of quantum gravity and provides a means for further investigation into fundamental physics. It applies to quantum modifications and more sophisticated thermodynamics of BHs.

The quantum effects can be considered as significant near a BH horizon; GUP interactions are critical for determining the dynamics of BHs. Quantum interactions, such as GUP interactions with thermodynamical features with different rotations of BH, have been studied using the quantum tunneling approach [28–37]. The modification rate of the Hawking temperature in BH evaporation is greatly influenced by quantum changes, which must be considered. However, there is no concrete scientific evidence to support the hypothesis; some predictive models indicate that a BH can stop radiating at its minimal mass, leaving behind a residue. Moreover, quantum processes are not immediately taken into account by regular BH metrics; thus, implementing quantum changes requires a detailed study of quantum-improved metrics and their implications. The quantum improved metric of Schwarzschild BHs was recently determined [38] by two effective field theory (EFT) approaches, which have also shown important discoveries in the field of quantum gravity. [39–45]. A logical quantum gravity at all scales of energy remains very fascinating; EFT approaches can be employed at energies below the Planck mass, allowing for model-free gravity in quantum operations. In the tunneling approach, the spin one particle of Hawking temperature was examined by Gecim and Sucu, which was crucial for the BH spacetime [46] and GUP frame [47–48]. The GUP framework demonstrated that temperature is affected by tunneled particles in addition to BH properties. The quantum spin of a relativistic particle and BH temperature of the particle vector bosons, as indic-

ated by the modified equation, form the foundation for their vector particle expressions. The GUP changes to the Euler–Heisenberg-AdS BH temperature have been computed by the newly modified equations [49]. The primary characteristics of the BH and its standard thermodynamics were examined, and the modified model was compared with the standard thermodynamics in specific particle physical properties. When the attractive Coulomb interaction was included in the consideration in [50], the efficiency that emerged from the GUP interaction for the zitterbewegung particles was higher than that achieved with the conventional temperature.

An emerging-gravity metric that includes a scalar field of k -essence has been combined with a Born-Infeld Lagrangian [51] and Dirac–Born–Infeld Lagrangian [52] to generate a metric that describes the geometry of a BH in a massive object. The Hawking temperature of the metric has been determined. In addition to verifying this quantum BH emission in the context of dark energy, the use of the Hamilton–Jacobi method to perform tunneling with both spin BH parameter and non-singular of non-spin BH in different coordinate structures demonstrates a new occurrence of reception in white holes through quantum physical tunneling [53]. Mitra explored emission tunnels across the BH horizon, which lead to a temperature that is twice as high as usual [54]. Contracted dark matter profiles with steeper inner slopes are seen in galaxy regions, suggesting increased central concentrations and possible ray characteristics from dark matter annihilation [55], and the formation of nonlinear structures in a two-field fuzzy dark matter model was examined [56]. Burkert predicted [57] the scaling interaction for fuzzy dark matter cores; the empirically derived scaling interaction between core size and virial mass was the opposite. In [58], the semi-analytical descriptions of the matter distribution in the non-linear regime illustrate the difficulty of predicted structure creation in models with mechanics not limited to collision-free dark matter.

Quantum modifications may have an impact on the entropy of BHs in thermodynamics. Quantum modifications consider changes generated by gravity quantum concepts, in contrast to thermal implications, which align with the standard thermodynamics of BHs, as described by the entropy of Bekenstein–Hawking. In an expanded strategy, both components are considered within a single structure. The quantum modifications to BH entropy were determined through extremely complex techniques that include loop quantum gravity [59], near-horizon symmetries, and Hamiltonian fracture functions [60]. A canonical entropy that provides for thermal fluctuations appropriate for logarithmic changes to BH entropy as micro-canonical entropy was investigated [61]. In accordance with thermodynamics, thermal fluctuations are prohibited in the horizon regions in an isolated horizon barrier, and no radiation can pass the horizon inside it. Considering that

the Schwarzschild BH has a specific heat, it is shown to be in equilibrium with temperature, which suggests that its entropy and thermal properties are appropriately described. The BH can be confined in a finite-radius cavity by simply immersing it in an isothermal bath, and the environment will ultimately attain equilibrium in terms of temperature. Bekenstein et al. detected a regularly spaced region spectral [62] from the literature. According to [63], the position of the observer impacts the local temperature for a stationary local observer. We deduce from a canonical boundary scenario that there may be two solutions or none at all. The specific heat increases with greater mass and decreases with reduced mass [63–64]. It has been explored how the greater mass resolution derived from a regularly spaced area spectrum occurrence alters the Schwarzschild BH. The context of Schwarzschild BH in a finite-sized, confined cavity was examined in [65] to achieve thermal equilibrium. Because of the logarithmic changes of thermal fluctuations related to entropy, the Schwarzschild BH never existed in the state of thermal equilibrium. Furthermore, the changed entropy has been analyzed, and the thermal properties correspond to stability considerations and the physical properties of various BH types based on modified correction factors [66–71]. The dynamics of BH geometries have been analysed by using GUP-deformed thermodynamics [72–78] and geodesics [79].

It is important to determine tunneling radiation in the outside horizon spacetime by implementing several confirmed techniques. However, T_H becomes even more significant as we examine the spacetimes in quintessence matter. The basic formula raises the BH standard T_H . The results we obtained indicate that T_H is significantly influenced by all of the quintessence matter contributions. In this analysis, we explore the T_H of a four-dimensional BH in the presence of quintessence matter. We also illustrate that the T_H is influenced by the quantum gravity of the BH. A Schwarzschild BH T_H is comparable to this T_H . Mass is reduced, and evaporation occurs as every particle releases the energy and mass that the BHs dropped due to Hawking radiation. Inside the rate uncertainty region, its radiation is released. This process explains the law of momentum and energy applied by the physics of relativity. This semi-classical approach can be equivalent to the derivative of the equation T_H , which merges the relativistic matter of the electric field BH from *GR* with the uncertainty principle from quantum mechanics. In physics, the Hamilton-Jacobi semi-classical approach is frequently employed for situations that offer various possibilities for explanation. However, this type of approach could generate assumptions that impact validity. The characteristics of quantum fields close to the horizon are crucial to our explanation of particle production. The appropriately disregarded self-attraction, self-gravity, and back-reaction constitute the particle's radi-

ation. The goal of this investigation is to explore the Hawking radiation that originates from the significant spacetime of vector particles in quintessence matter. The Standard Model includes significant emphasis on particles (spin one bosons), such as the well-known W^\pm bosons [7, 80]. When we consider the massive bosons in space-time, the motion of the boson field can be stated by the Lagrangian expression. In this case, we can examine the tunneling mechanism using the Hamilton-Jacobi semi-classical procedure, employing a Lagrangian formulation with a WKB approximation in space-time, which is comparable to the technique in [7]. The analysis of the motion of the different fields is more complicated in the Lagrangian formulation due to the interaction of quintessence matter. First, we derive the W^\pm boson field expression through the Lagrangian of the Glashow-Weinberg-Salam model. In the framework of quintessence matter, we solve the following equation in spacetime using the semi-classical and WKB approximation. Setting the coefficient of the matrix determinant to zero enables us to calculate the linear expression for the radial function. We investigate the tunneling rate related to the Hawking temperature, which represents the significant spacetime of vector particles in quintessence matter, and obtain the corresponding entropy and emission energy.

The prospective applicability of our approach to astrophysics is illustrated by examining the existence of observational data. Hawking-like radiation impacts and BH dynamics are indirectly demonstrated by observations of BH applications employing detections of gravitational waves (e.g., LIGO and Virgo) and high-energy waves (e.g., Event Horizon Telescope). However, accurate evaluations of Hawking radiation remain difficult due to its weak signal relative to the visible electromagnetic field. This result validates efforts to use scientific models such as gravity and the GUP to introduce quantum modifications to comprehend these empirical data.

In the present study, we explore T_H via a conventional formula and investigate BHs in quintessence matter, as outlined in Sec. II. In Sec. III, the tunneling radiation is presented. For the correction of T_H , which changes physical stability and instability, graphics are examined. We explain corrected entropy in Sec. IV and GUP-corrected emission energy in Sec. V. We conclude our paper in Section VI.

II. BLACK HOLE SOLUTION IN QUINTESSENCE MATTER

For the spherically symmetric, static basic state of a BH, which is encircled by a field, Kiselev found [81] the exact solutions to Einstein's formulations. These suggestions were constructed on the energy-momentum tensor of quintessence's distinct intrinsic configuration and the state component ω . The contributions to the general en-

ergy-momentum tensor, along with the appropriate additivity and linearity criteria, generated linear formulations for the various matter terms. It derives precise limitations on the known solutions for different fields, suggesting the relativistic significance of the pressure and density of quintessence matter. Belhaj *et al.* [82] studied the effects of dark energy on the properties of BHs by considering a surrounding quintessence field and expanding the BH solutions to investigate the manner in which the quintessence parameter and associated equation of state affect BH horizon structure and thermodynamic behaviour. To demonstrate that dark energy has a considerable impact on the position of event and cosmic horizons and obtain the main metric, we start from the Einstein field equations

$$G_{\mu\nu} = 8\pi T_{\mu\nu}, \tag{1}$$

for a static and spherically symmetric spacetime

$$ds^2 = e^{\nu(r)} dt^2 - e^{\lambda(r)} dr^2 - r^2(d\theta^2 + \sin^2\theta d\phi^2). \tag{2}$$

The independent Einstein equations for this metric are [83]

$$2T^t_t = -e^{-\lambda} \left(\frac{1}{r^2} - \frac{\lambda'}{r} \right) + \frac{1}{r^2}, \tag{3}$$

$$2T^r_r = -e^{-\lambda} \left(\frac{1}{r^2} - \frac{\nu'}{r} \right) + \frac{1}{r^2}, \tag{4}$$

$$2T^\theta_\theta = 2T^\phi_\phi = -\frac{1}{2} e^{-\lambda} \left(\nu'' + \frac{\nu'^2}{2} - \frac{\nu' - \lambda'}{r} - \frac{\nu'\lambda'}{2} \right). \tag{5}$$

The surrounding matter is modeled as a quintessential anisotropic fluid

$$T^t_t = T^r_r = \rho_q(r), \quad T^\theta_\theta = T^\phi_\phi = -\frac{1}{2} \rho_q(3w_q + 1), \tag{6}$$

where w_q is the state parameter. Subtracting the tt and rr equations gives

$$\nu'(r) + \lambda'(r) = 0, \tag{7}$$

where $e^\nu = e^{-\lambda} \equiv F(r)$. Defining $e^{-\lambda} = 1 + F(r)$, one obtains

$$r^2 F'' + 3(1 + w_q)rF' + (3w_q + 1)F = 0. \tag{8}$$

Solving this differential equation yields

$$F(r) = 1 - \frac{2M}{r} - \frac{C_q}{r^{3w_q+1}}, \tag{9}$$

which leads to

$$ds^2 = -F_{tt}(r)dt^2 + \frac{1}{G_{rr}(r)}dr^2 + r^2d\theta^2 + r^2\sin^2\theta d\phi^2, \tag{10}$$

with

$$F_{tt}(r) = G_{rr}(r) = 1 - \frac{2M}{r} - \frac{C_q}{r^{1+3w_q}}, \tag{11}$$

where C_q is a quantity associated with the quintessence matter density [84]

$$\rho_q = -\frac{3C_q w_q}{2r^{3(1+w_q)}}. \tag{12}$$

The recovery of the Schwarzschild BH occurs when $C_q = 0$. Dust is expressed by $P_q = w_q \rho_q$. $w_q = 0$, which is equivalent to dust, is a matter parameter that connects density and pressure. Here, the charged BH solution is re-created, where $w_q = \frac{1}{3}$ is the electric field of relativistic matter. In the AdS context, the BH solution appears with $w_q = -1$, which is the cosmological constant. Because the quintessence dark matter is represented by $-1 < w_q < 0$, quintessence implies negative pressure.

The parameter (w_q) indicates the equation of state of the quintessence (dark energy) field around the BH. If $-1 < w_q < -\frac{1}{3}$, the quintessence is extremely repulsive at great distances, creating an outer horizon at $r = r_+$, analogous to a cosmological (de Sitter) horizon. If $-\frac{1}{3} < w_q < 0$, the repulsion is less and influences the BH solution interior, forming an inner horizon $r = r_-$ of BH type. The value of w_q determines if the horizon is a BH solution.

The standard formula found in the scientific literature can be used to determine the T_H for BH spacetime in the interpretation of quintessence matter with BH surface gravity $K(r_+)$. T_H can be expressed as

$$T_H|_{r=r_+} = \frac{1}{4\pi} \left[\frac{2M}{r_+^2} + (1 + 3w_q) \frac{C_q}{r_+^{2+3w_q}} \right]. \tag{13}$$

T_H depends on the quintessence matter density-related parameter (C_q), BH outer radius (r_+), matter state parameter, and BH mass. When $C_q = 0$ and $r_+ = 2M$, we get the Schwarzschild temperature $T_{(Sch.)} = \frac{1}{8M\pi}$, which is comparable to our first term of T_H .

In Fig. 1(i), all plotted curves decrease monotonically, confirming the familiar inverse-size relationship of BH

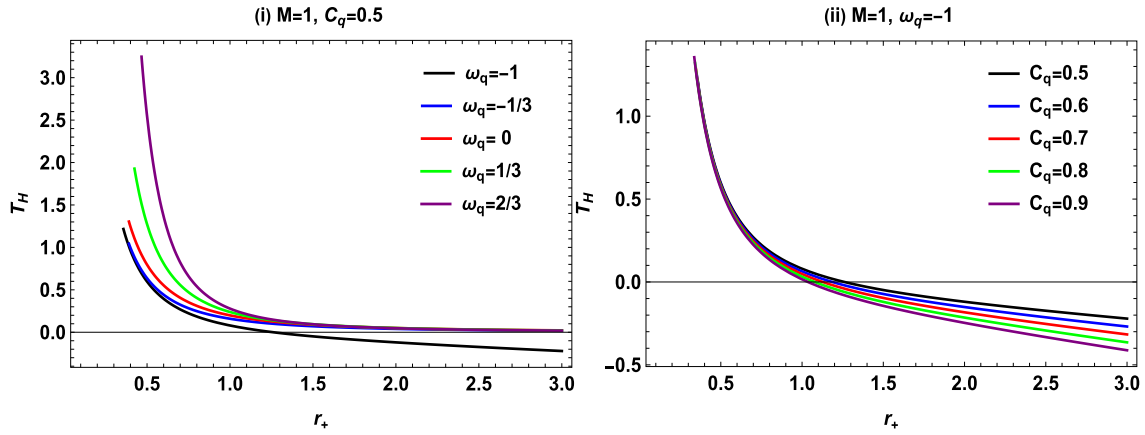


Fig. 1. (color online) Temperature T_H via horizon radius r_+ with fixed mass $M = 1$ for varying values of state parameter ω_q and density parameter C_q .

temperature: hotter BHs are formed at smaller event horizons and colder BHs at larger event horizons. The temperature dependence on the value of ω_q is most pronounced at smaller event horizons and becomes less relevant at larger event horizons, where the temperature curves consolidate. For models with larger and, thus, less negative values of ω_q , the temperature becomes significantly higher near the event horizon and produces a steeper drop-off. For more negative values of ω_q , the temperature suppression becomes much more prominent and the temperature profile becomes more level. That is, the quintessence equation of state most directly impacts near-horizon thermodynamics and the corresponding short-time evaporation characteristics, affecting the larger, effectively classical, macro realm much less.

As shown in Fig. 1(ii), modifying quintessence density can move the whole temperature profile up or down without significantly changing the form. Larger C_q uniformly suppresses T_H at all plotted radii. At the same time, a smaller C_q allows all radii to attain higher temperatures, with the most remarkable absolute differences, once again, at small r_+ . The temperature is significantly reduced and, for large enough density, crosses into low (or negative) values in the small radius zone, which means that a strong-quintessence background cools and stabilizes the BH against fast evaporation. Briefly, while ω_q alters the gradients and small radius peak structures of T_H , C_q behaves as a scalar control over the temperature scale. Thus, the two parameters complement each other in controlling thermodynamic stability at the BH's nearest horizon.

III. TUNNELING RADIATION IN BLACK HOLE WITHIN QUINTESSENCE MATTER

String theory, loop quantum gravity, and non-commutative metric comprise many hypotheses of quantum

gravity, which possess a minimal definable length [85–88]. This smallest length can be achieved with the GUP [89–91]. A successful model of the GUP, which includes the central idea of enormous further dimensions in single-dimensional quantum theory, has been proposed [92] as

$$L_F K_i(P) = \tanh\left(\frac{P}{M_F}\right), \quad (14)$$

$$L_F \omega_1(E) = \tanh\left(\frac{E}{M_F}\right). \quad (15)$$

The wave vector K_i indicates operators of the spacetime modifications, and frequency ω_1 also indicates operators of the spacetime modifications, whereas L_F and M_F represent the larger-dimensional lowest length and Planck mass, respectively. Consequently, we get L_F and M_F satisfying $L_F M_F = h$. The quantization of position description $\hat{x} = x$ provides

$$\omega_1 = i\partial_t, \quad K_i = -i\partial_x. \quad (16)$$

Thus, by considering the order of $\left(\frac{P}{M_F}\right)^3$, the low energy limit $P \ll M_F$ gives

$$E \simeq i\hbar\partial_t \left(1 - \delta\hbar\partial_t^2\right), \quad (17)$$

$$P \simeq -i\hbar\partial_x \left(1 - \delta\hbar\partial_x^2\right), \quad (18)$$

with $\delta = \frac{1}{3M_F^2}$. The transformed commutation connection can be illustrated by

$$[x, P] = i\hbar(1 + \delta P^2), \tag{19}$$

and the generalized uncertainty's relationship is

$$\Delta x \Delta P \geq \frac{\hbar}{2} [1 + \delta(P^2)]. \tag{20}$$

Eqs. (19) and (20) visibly demonstrate that GUP deviation from the Heisenberg uncertainty principle rises with the particle's momentum. Consider that Eqs. (17)–(20) are limited to the precise scenario studied in this case, notably, the low-energy limit $P \ll M_F$. To verify the uncertainty principle, demonstrations such as those suggested by [93–94] should limit the parameter δ to the minimal energy space. Further generalized uncertainty coincidences have been found in previous analyses. We explore how massive one-spin particles penetrate across BH horizons via the Hamilton–Jacobi algorithm, which considers the smallest length impact by Eqs. (17) and (18). According to these predictions, the mass of the BH, mass of the boson particles, and angular momentum of the boson particles that are discharged are related to the quantum gravity evolution. The quantum transformation will eliminate the standard action for a temperature rise at a specific point during evaporation, which leads to the generation of remnants. It also explicitly delays the temperature rising through the BH evaporation mechanism.

We explored particle tunneling exceeding a space-time horizon via the Lagrangian formulation. According to the real and imaginary computations, the mass of the particle alters the transformed T_H for the tunneling of a vector particle. Ignoring the low value component in the quadratic root expression with significance in nature reveals that the T_H of spacetime depends on both the expelled particle mass and kinetic energy. The realistic calculation indicates that the quintessence matter of the expelled particle determines the T_H for vector tunneling through space-time. We start with the kinetic factor of the uncharged flat spacetime with boson field under the framework of the GUP. The adjusted field strength tensor $\frac{1}{2} \tilde{B}_{\mu\nu} \tilde{B}^{\mu\nu}$ is implied by [7]

$$\tilde{B}_{\mu\nu} = (1 - \delta h^2 \partial_\mu^2) \partial_\mu B_\nu - (1 - \delta h^2 \partial_\nu^2) \partial_\nu B_\mu. \tag{21}$$

Covariant derivatives are also required due to the gauge principle; the further derivative affects the local unitary transform operator $U(x)$ [95]. It should be noted that there are other derivative terms. The boson field (W^\pm) in BH spacetime is generalized as

$$(1 - \delta h^2 \partial_0^2) \partial_0 \rightarrow (1 + \delta h^2 F_{tt}^{00}(r) \nabla_0^{\pm 2}) \nabla_0^\pm, \tag{22}$$

$$(1 - \delta h^2 \partial_i^2) \partial_i \rightarrow (1 - \delta h^2 F^{ii}(r) \nabla_i^{\pm 2}) \nabla_i^\pm. \tag{23}$$

The geometrical covariant derivative is represented by ∇_μ . The variation in signs of the $O(\delta)$ factor in Eqs. (22) and (23) can be explained by the fact that $F_{tt}^{00}(r)$ and $F^{ii}(r)$ always have different signs. By defining

$$\nabla_o^\pm = (1 + \delta h^2 F_{tt}^{00}(r) \nabla_o^{\pm 2}) \nabla_o^\pm, \quad \nabla_i^\pm = (1 - \delta h^2 F^{ii}(r) \nabla_i^{\pm 2}) \nabla_i^\pm. \tag{24}$$

The Lagrangian GUP-deformed expression for the W -vector field is [7]

$$L^{\text{GUP}} = -\frac{1}{2} (\nabla_\mu^+ W_\nu^+ - \nabla_\nu^+ W_\mu^+) (\nabla^{-\mu} W^{-\nu} - \nabla^{-\nu} W^{-\mu}) - \frac{m_W}{\hbar} W_\mu^+ W^{-\mu}. \tag{25}$$

Therefore, it is crucial to take sufficient general action as

$$S^{\text{GUP}} = \int d^4x \sqrt{-F} L^{\text{GUP}} (W_\mu^\pm, \partial_\mu W_\nu^\pm, \partial_\rho \partial_\mu W_\nu^\pm, \partial_\rho \partial_\mu \partial_\lambda W_\nu^\pm), \tag{26}$$

with F being a coefficient of metric (10). Consideration is given to the Lagrangian GUP-deformed expression and its physical significance. The singularity-free field equation is transformed as a Lagrangian GUP-deformed expression. We investigate the boson radiation phenomena via the vector field in the GUP-deformed expression of action as

$$\begin{aligned} \partial_\mu (\sqrt{-F} W^{\nu\mu}) + \sqrt{-F} \frac{m^2}{\hbar^2} W^\nu + \delta h^2 \partial_0 \partial_0 \partial_0 (\sqrt{-F} F^{00} W^{0\nu}) \\ - \delta h^2 \partial_i \partial_i \partial_i (\sqrt{-F} F^{ii} W^{i\nu}) = 0. \end{aligned} \tag{27}$$

In this particular case, F , $W^{\nu\mu}$, and m denote the antisymmetric tensor, boson particle mass, and coefficient matrix determinant, respectively. The antisymmetric tensor is defined as

$$W_{\nu\mu} = (1 - \delta h^2 \partial_\nu^2) \partial_\nu W_\mu - (1 - \delta h^2 \partial_\mu^2) \partial_\mu W_\nu, \tag{28}$$

where the GUP parameter is represented by δ , while Planck's constant is \hbar . The components of W^μ and $W^{\mu\nu}$ should be calculated as

$$W^0 = -\frac{1}{F(r)} W_0, \quad W^1 = G(r) W_1,$$

$$\begin{aligned}
 W^2 &= \frac{1}{r^2} W_2, \quad W^3 = \frac{1}{r^2 \sin^2 \theta} W_3, \\
 W^{01} &= -W_{01}, \quad W^{02} = -\frac{1}{F(r)r^2} W_{02}, \quad W^{03} = -\frac{1}{F(r)r^2 \sin^2 \theta} W_{03}, \\
 W^{12} &= \frac{F(r)}{r^2} W_{12}, \quad W^{13} = \frac{G(r)}{r^2 \sin^2 \theta} W_{13}, \quad W^{23} = \frac{1}{r^4 \sin^2 \theta} W_{23}.
 \end{aligned} \tag{29}$$

The examination of BHs in quintessence matter is an important area of the framework of quantum gravity implications, and many BH physics experiments have made use of the GUP. The dynamics of BHs have been examined in the framework of the GUP [7]. Through the integration of the GUP with the tunneling algorithm, the tunneling modified probability of a Schwarzschild BH was examined by Nozari and Mehdipour [96]. The Hamilton–Jacobi GUP-deformed model for bosons in curved spacetime was presented in [80], along with the corrected Hawking temperatures calculated for various spacetime types. Although this attribute naturally results in a reduced mass during the evaporation of the BH in dark matter, the effects of quantum gravity were found to slow the increase in Hawking temperatures, as determined by boson tunneling analysis. It is stated by [97] that, according to the WKB technique,

$$W_\nu = c_\nu \exp \left[\frac{i}{h} H_0(t, r, \theta, \phi) + \Sigma h^n H_n(t, r, \theta, \phi) \right], \tag{30}$$

where c_ν reflects the constant term, and (H_0, H_n) corresponds to arbitrary functions. We generate the equation system presented, disregarding higher orders in the Lagrangian GUP-deformed expression (26) and just incorporating the term h in the WKB approximation for the 1st order. We obtain the set of field expressions in **Appendix A**. We consider the variable split phenomenon as

$$H_0 = -Et + W(r, \theta) + J\phi, \tag{31}$$

with $E = (\tilde{E} - J\Omega)$, where J , Ω , and \tilde{E} denote the boson particle angular momentum, boson particle angular velocity, and energy at angle ϕ , respectively. We set K in **Appendix B** to zero and ensure that the imaginary portion operates as described, provided that the K determinant is non-trivial.

$$\text{Im}W^\pm = \pm \int \sqrt{\frac{E^2 + R_1 \left[1 + \delta \frac{R_2}{R_1} \right]}{G(r)}} dr, \tag{32}$$

where $R_1 = \frac{J^2}{r^2}$ and $R_2 = \frac{\delta E^4}{F(r)} - G(r)\delta W_r^4 + \frac{\delta J^4}{r^2} + m^2$ illus-

trate the horizon's angular velocity. Equation (29) can be integrated around the pole to obtain

$$\text{Im}W^+ = \pi \frac{E}{2K(r_+)} [1 + \Xi\delta], \tag{33}$$

where Ξ denotes the tangent plane of kinetic energy factor in the horizon surface at the point where the radiation was created, and $K(r)$ denotes the BH in quintessence matter surface gravity. Pair formation is suggested as a mathematical explanation for tunneling radiation. The two particles in a pair may be separated in a region with strong gravitational pulls because they can annihilate at the same time. According to quantum physics, annihilation happens when a negative particle tunnels within the BH and a positive particle tunnels outside (radiation). For boson particles, the raised tunneling rate (T) can be determined as

$$T(W^+) = \exp[-4\text{Im}W^+] = \exp\left[-2\pi \frac{E}{K(r_+)}\right] [1 + \Xi\delta]. \tag{34}$$

Gravity pulls outer matter into BH in quintessence matter, which are regions of intense gravitational attraction. According to the traditional explanation, no energy can escape the BH in quintessence matter, not even electromagnetic waves, considering the strength of gravity. A BH, claimed to be Hawking, is a celestial object that emits radiation as a result of quantum events. The physical description of this emission mechanism is that these particles of positive mass and antiparticle of negative mass pairs are driven into the horizon of the BH in quintessence matter by vacuum fluctuations. We discovered that a negative particle mass would fall into the BH in quintessence matter, and a photon with positive energy has sufficient power to escape the BH in quintessence matter. The mass of the BH in quintessence matter eventually decreases as a function of the fall of a negative-energy particle. Moreover, an imaginary particle could be considered as thermal radiation. Two types of particles emerge from vacuum in this mechanism, which is known as a quantum tunneling effect. The particles tunnel across the horizon, exhibiting a complex action that resembles Hawking radiation caused by their positive energy. The charge, quintessence matter, mass, and directional momentum of the BH all impact the reflected radiation. Thus, in the context of gravity, the Hawking temperature for spacetime can be found through the application of the Boltzmann factor $T_W = \exp[-E/T'_H]$ in the GUP factor impact as

$$T'_H|_{r=r_+} = \frac{1}{4\pi} \left[\frac{2M}{r_+^2} + (1 + 3w_q) \frac{C_q}{r_+^{2+3w_q}} \right] [1 - \delta\Xi]. \tag{35}$$

This demonstrates how the spacetime structure and

quantum corrections modify T'_H . The zero-order, semi-classical, and fundamental Hawking correction factors are identical. To continue to satisfy GUP, the first-order correctable term must be less than the preceding term. The quintessence matter density-related parameter (C_q), BH outer radius (r_+), matter state parameter, and BH mass, as well as the GUP parameter, all affect T'_H . Additionally, we may determine the initial temperature of the spacetime within the context of the quintessence matter by setting the gravity parameter $\delta = 0$. The Hawking temperature of BH spacetime in quintessence matter is obtained when $\delta = 0$. When $C_q = 0$ and $r_+ = 2M$, we get the Schwarzschild temperature $T_{(Sch.)} = \frac{1}{8M\pi}$, which is comparable to our first T_H term. The reduction of dimensions at the horizon can be used to study the typical mechanisms of particle tunneling [98–99]. All massive, non-extremal BHs are essentially similar to the Rindler space. By incorporating infinite blueshift, all particle types at the horizon for the usual Hawking radiation appear to be massless, leading to particles with a Hawking temperature. Our findings also show that the quantum interactions of gravity should result in different desired Hawking temperatures for particles with distinct identities or number structures. As the particles approach the horizon, the existence of a minimal length prevents them from ever having experienced an infinite blueshift. In the case of quintessence matter, the quantum gravity contribution in the T_H of a spacetime in quintessence matter is irregular. Ξ denotes an expression of θ as follows:

$$\Xi = 6 \left(\frac{J_\phi^2 \csc^2 \theta + J_\theta^2}{r_+^2} + m^2 \right) > 0. \quad (36)$$

The $\csc^2 \theta$ term causes the visible divergence of Ξ at $\theta = 0, \pi$, which is not a real singularity but more of a coordinate illusion of spherical coordinates. The azimuthal angular momentum J_ϕ must vanish at $\theta = 0, \pi$ for the

wave function to be regular on the polar axis. This implies that the combination $J_\phi^2 \csc^2 \theta$ stays finite. Additionally, the tunnelling analysis relies only on the radial portion of the action and is carried out locally close to the event horizon. As a result, any coordinated singular behaviour at the poles does not contribute to the tunnelling probability or Hawking temperature. Therefore, in the physically significant region, Ξ remains finite and strictly positive.

In Fig. 2(i), all combinations display the same patterns when observing the falling limit of the corrected temperature T'_H . As the curves approach the small radius region, they become more sensitive to any changes made to the parameters. In contrast, for larger r_+ values, the curves align to a standard low temperature. Modifying ω_q affects the amplitude and steepness of the temperature close to the horizon. Models characterized by larger, less negative ω_q values and small r_+ values exhibit a much steeper temperature drop, while more negative ω_q values result in a small radius temperature. More importantly, the quintessence equation of state impacts small-scale thermodynamic behavior, indicating the initial stages of evaporation. ω_q governs the temperature rise at small scales, while the larger, quasi-classical region remains relatively unchanged.

In Fig. 2(ii), altering the GUP parameter results in changes to the temperature profile in a qualitatively different manner: temperature values around the horizon in the case of higher δ are more suppressed, and the peak becomes more gentle as r_+ grows. The most important effect of a larger δ is the regularization of the small radius behaviour; this restricts the extreme rise (or divergence) of the classical temperature, so the curves approach a finite, low value rather than diverging to infinity. This behavior means that GUP corrections work as a universal damping or stabilising mechanism in the evaporating BH, reducing thermal emission at small radii and encouraging remnant behaviour. Hence, in conjunction with ω_q , δ per-

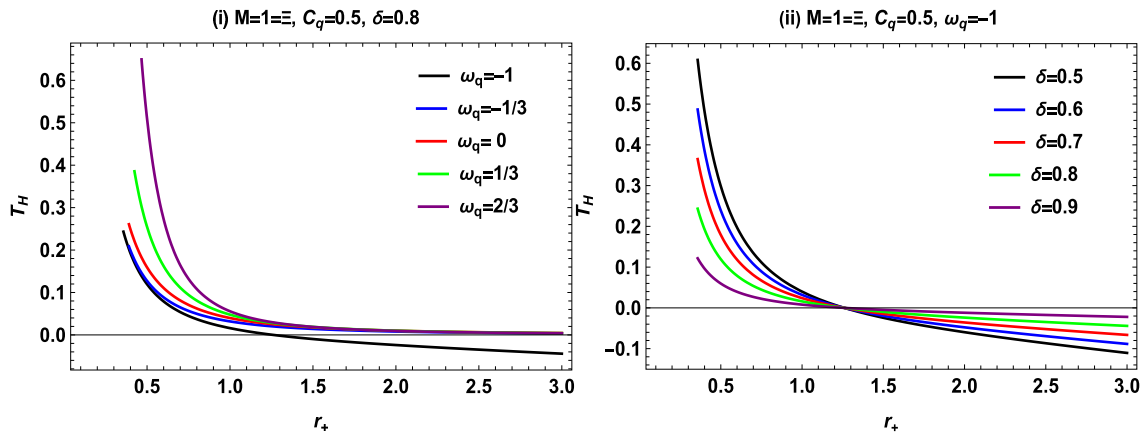


Fig. 2. (color online) Corrected temperature T'_H via horizon radius r_+ with fixed $M = 1 = \Xi$ and $C_q = 0.5$ for varying values of state parameter ω_q and GUP parameter δ .

forms the function of a regulator (scaling and smoothing temperatures) while controlling the detailed gradient and near-horizon sensitivity, whereas ω_q determines the rapid quantum-dominated evaporating path, stabilizing at a low temperature remnant. Equation (33) can be inserted into Eq. (32) to obtain the modified temperature as

$$T'_H|_{r=r_{\pm}} = \frac{1}{4\pi} \left[\frac{2M}{r_{\pm}^2} + (1 + 3w_q) \frac{C_q}{r_{\pm}^{2+3w_q}} \right] \times \left[1 - 6\delta \left(\frac{J_{\phi}^2 \csc^2 \theta + J_{\theta}^2}{r_{\pm}^2} + m^2 \right) \right]. \quad (37)$$

T'_H is associated with the dark matter fields that surround the BH. Further, the temperature growth throughout evaporation is specifically opposed by quantum procedures, which progressively bring the temperature back to equilibrium. There will definitely be a BH remaining. The tunneling methodology is interesting for predicting the BH temperature because it provides an interactive model of the BH radiation that includes multiple features. When exploring the BH evaporation mechanism without including back-reaction implications, a strategy is very helpful. Multiple approaches to determining the fundamental characteristics of BHs have been shown to be feasible and carefully consider the dynamic nature of the radiation. One of the tunneling strategy's unique features is its applicability to studying the impact of quantum gravity on black hole radiation. When particle pairs are formed inside the horizon, one of them can tunnel quantumly through the BH horizon in accordance with the tunneling formalism. It seems more reliable that certain aspects of the internal structure of the BH, such as the impacts of quantum gravity, may be displayed in its radiated and perceived visible light to outside observers.

For the dust field, electric relativistic matter field, cosmological constant, and quintessence dark matter, the Hawking temperature is specified as $0.2 \leq r_+ \leq 0.4$. Furthermore, as summarized in Table 1, the quintessence matter behaves positively with Hawking temperature, evaluating the first law of thermodynamics. In the context of the relative dust field, electric relativistic matter field, cosmological constant, and quintessence dark matter, we can conclude that the ideal temperature is more

prominent than the modified temperature. We utilized the data presented in Table 1 to investigate the quantum gravity reflection in relation to lowering the temperature. In BH thermal dynamics, a lower temperature indicates changes between various field states, which generally correspond with quantum gravity interactions. This corresponds to a state of thermodynamic equilibrium where phenomena such as GUP corrections become important. It is vital to study temperature, entropy, and emission energy corrections under quantum gravity effects, which also offer information about the complex dynamic nature of BHs. Table 2 presents the variation of the modified Hawking temperature T'_H with the GUP parameter δ from 0 to 0.05, illustrating the impact of quantum modifications. It also shows the impact of quintessence normalisation C_q on the outer (r_+) horizons. The impacts of w_q , C_q , and δ on T'_H are clearly indicated. Observations explain the physical characteristics of the horizon and how these parameters affect temperature. The key typical values of w_q (1/3, 0, -0.5, and -1) cover the relativistic matter, dust, quintessence, and cosmological constant situations. Overall, Table 2 presents an all-inclusive view of how essential fields and BH modifications alter BH dynamics.

In Fig. 3(i), the corrected temperature shows sharp decreases while gaining larger horizon radii and exhibits an inverse relationship that is characteristic of BH thermodynamics. When δ is increased, the temperature value increases from a lower magnitude overall. This means that the effect of quantum gravity is stronger, and the thermal behavior is enhanced near smaller horizons. The temperature value is highly sensitive to δ , as indicated by the dense clustering of contour lines and smaller radii. The weaker influence, with spread at larger radii, suggests that GUP corrections near the thermal profile of the horizon essentially shift the smaller quantum near BHs.

In Fig. 3(ii), corrected temperature horizons with a similar descending behavior across radii show the shifted influence pattern and degree with ω_q and the shifted amplitude and gradient. Temperature contour lines shifting upwards indicate higher thermal intensity and slower decay as ω_q increases, representing positive scales of ω_q . This describes a BH of intense thermodynamic activity, characterized by less exotic dark energy and a more positive expansion of dark energy. The remarkable variation in

Table 1. $M = 1$ and $\Xi = 1$ remain constant, but T_H and T'_H are apparent for various fields at various values of quintessence matter density-related parameter (C_q), quintessence matter density ρ_q , and GUP (δ) parameter. Different locations make up the event horizons; we only take the outer horizon values as $0.2 \leq r_+ \leq 0.4$.

w	r_+	ρ_+	C_q	T_H	δ	T'_H
$w = 0$ (Dust field)	$2M_{Sch.}$	0.0	0.0000	≈ 15.915	0.5	≈ 7.958
$w = \frac{1}{3}$ (Radiation Field Relativistic Matter)	0.2	1.0	-0.0032	≈ 3.915	0.6	≈ 1.566
$w = -1$ (Cosmological Constant)	0.3	1.1	0.7333	≈ 1.734	0.7	≈ 0.520
$-1 < w < 0$ (Quintessence Dark Matter)	0.4	1.5	0.506	≈ 0.963	0.8	≈ 0.193

Table 2. T'_H for different values of w_q , C_q , δ , and outer (r_+) horizon. Parameters: $\Xi = 1$ and $M = 1$.

w_q	C_q	δ	r_+	T'_H	Remarks
1/3	0.10	0.00	1.80	0.092	Radiation field, no GUP
		0.01	1.80	0.091	Small GUP correction
		0.05	1.80	0.087	Strong GUP suppression
0	0.10	0.00	2.00	0.080	Dust background, Schwarzschild limit
		0.01	2.00	0.079	Small δ correction
		0.05	2.00	0.076	Large δ correction
-0.5	0.10	0.00	2.15	0.073	Quintessence-dominated spacetime
		0.01	2.15	0.072	Small GUP effect
		0.05	2.15	0.069	Enhanced quantum gravity correction
-1.0	0.10	0.00	2.25	0.068	Cosmological constant dominated
		0.01	2.25	0.067	Small δ effect
		0.05	2.25	0.063	Strong GUP suppression

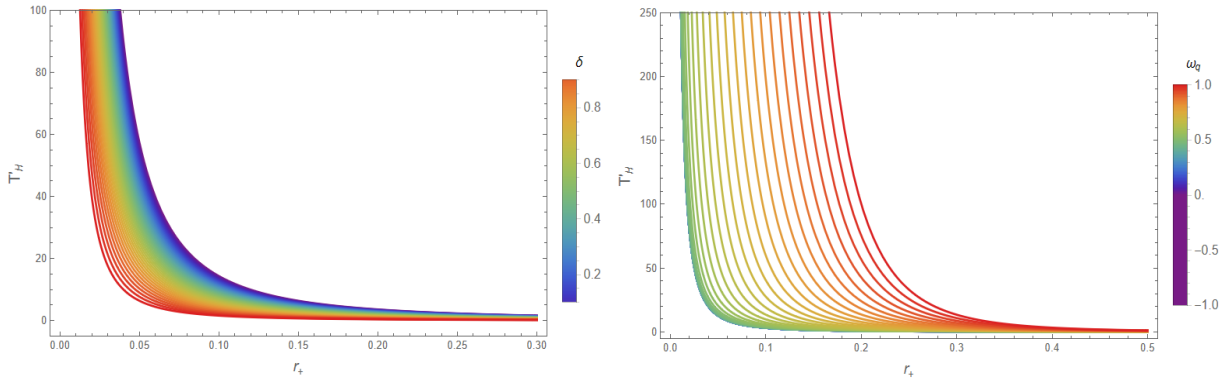


Fig. 3. (color online) Corrected temperature T'_H via horizon radius r_+ with fixed $M = 1 = \Xi$ and density $C_q = 0.5$ for varying values of GUP parameter δ with state parameter $\omega_q = -1$ and for varying values of state parameter ω_q with fixed GUP parameter $\delta = 0.8$.

smaller radii is a result of strong bonding with the dark energy of the state parameter, BH thermodynamics, and its GUP effect.

IV. ENTROPY CORRECTIONS TO BLACK HOLE IN QUINTESSENCE MATTER

Analyzing entropy corrections reveals how gravitational, quantum, and astrophysical phenomena interact in complex systems. In classical general relativity, the BH entropy is determined by the area of the event horizon, and the BH entropy area relation, Bekenstein-Hawking, is claimed as the BH area entropy theorem. In contrast, in realistic astrophysical situations, especially those affected by dark matter, this relationship is significantly modified. Dark matter's gravitational influence alters the spacetime geometry around the BH, affects its thermodynamic equilibrium, and drives entropy changes due to statistical and quantum corrections. In particular, they arise from the GUP, quantum gravity effects, or changes to the quintessence matter's density profile. The study of

these corrections in entropy improves the understanding of the thermodynamics of BHs in non-vacuum spacetimes and how dark matter modifies fundamental properties such as BH temperature, stability, evaporation, and entropy. Therefore, analogous to the study on free dust, this study on entropy correction connects the quantum description of gravity to the astrophysics of a universe dominated by dark matter. Furthermore, the classical Boltzmann entropy has logarithmic corrections to improve it in statistical mechanics, and in the quantum system, quantum fluctuations and finite-size effects are also considered [100]. Banerjee and Majhi examined the entropy corrections with the help of the strategy of null geodesics [101–103]. To obtain the corrected entropy of BHs in quintessence matter, we apply the formula of Bekenstein-Hawking entropy first-order corrections. The logarithmic corrected entropy S_H of the BH in quintessence matter can be calculated using the formula

$$S_H = S_{H_0} - \frac{1}{2} \ln \left| T_H'^2 S_{H_0} \right| + \dots \tag{38}$$

The standard entropy for a BH in quintessence matter can be calculated by the formula

$$\mathbb{S}_{H_0} = \frac{A_H}{4}, \quad (39)$$

where

$$A_H = \int_0^{2\pi} \int_0^\pi \sqrt{g_{\theta\theta}g_{\phi\phi}} d\theta d\phi = 4\pi r^2. \quad (40)$$

Substituting Eq. (37) into Eq. (36), the standard entropy for a BH in quintessence matter can be obtained as follows:

$$\mathbb{S}_{H_0} = \pi r_+^2. \quad (41)$$

After inserting the values from Eqs. (38) and (32) into Eq. (35), we compute the corrected entropy in the form

$$\begin{aligned} \mathbb{S}_H = \pi r_+^2 - \frac{1}{2} \ln \left| \frac{1}{16\pi} \left(\frac{2M}{r_+} + (1+3w_q) \frac{C_q}{r_+^{1+3w_q}} \right)^2 (1-\delta\Xi)^2 \right| \\ + \dots \end{aligned} \quad (42)$$

The above expression gives the corrected entropy for a BH in quintessence matter. It depends on the density-related parameter (C_q), BH outer radius (r_+), matter state parameter ω_q , BH mass M , GUP parameter δ , and arbitrary parameter Ξ .

In Fig. 4(i), the corrected entropy appears to rise almost linearly with the horizon radius at first, but around some critical radius, it sharply starts to diverge. This sort of behavior is superficially similar to a thermodynamic instability or phase transition, but one should not take this

divergence as an actual physical phase transition. Rather, it is an indication of the breakdown of the perturbative scheme used to accommodate the GUP and dark energy corrections. The range of values for ω_q also affects the magnitude of the entropy. When ω_q is negative, the entropy is greater as ω_q moves into positive territory, signifying that the state parameter of dark energy profoundly affects the rate at which entropy increases. The situation for $\omega_q = -1$ is exceptional, as a more negative ω_q (indicative of stronger dark energy dominance) increases the BH thermodynamic disorder and quantum corrections more significantly.

In Fig. 4(ii), the horizon radius gives rise to increased entropy for all values of δ . However, it does hit a peak and then levels out, signifying that the quantum gravity corrections become dominant. The relatively close spacing of the curves implies that the critical radius is where the parameters of δ take effect. The dominant GUP influence is within the small horizon limit, where quantum fluctuations are most active. This is where the close spacing of the curves indicates that δ parameters are most impactful near the critical radius.

V. EMISSION ENERGY CORRECTIONS FOR A BLACK HOLE IN QUINTESSENCE MATTER

We illustrate how energy emission rates depend on quintessence matter and quantum gravity. Furthermore, the creation and destruction of specific particle pairs near the horizon's limits allow positive-energy particles to escape the BH in quintessence matter through tunneling in the region where Hawking radiation occurs. The BH in quintessence matter evaporates due to this tunneling mechanism in the form of Hawking radiation. It has been demonstrated that for a far-off observer, its absorption cross-section reaches the BH shadow with quintessence

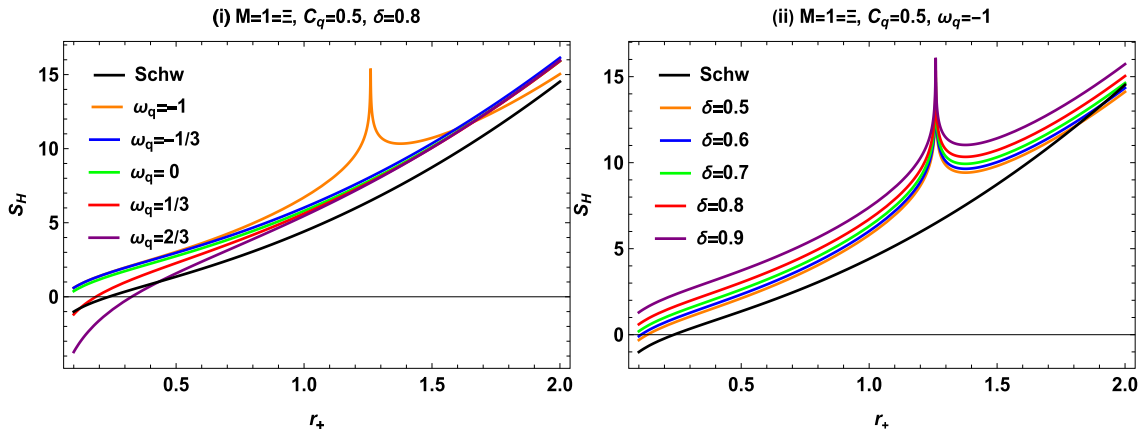


Fig. 4. (color online) Corrected entropy S_H as a function of horizon radius r_+ for varying values of state parameter ω_q and GUP parameter δ .

matter. The absorption cross-section fluctuates around a limiting constant (L_c) and a comparable photon radius, as indicated by Refs. [104–108]. The absorption cross-section exhibits the following characteristics:

$$L_c \approx \pi R^2, \quad (43)$$

where the symbol R represents the BH shadow radius in the context of quintessence matter, and the energy emission rate is expressed as follows:

$$\frac{d^2 E}{dt d\omega_p} = \frac{2\pi^2 \omega_p^3 L_c}{\exp\left(\frac{\omega_p}{T'_H}\right) - 1}, \quad (44)$$

where T'_H , $E = \frac{d^2 E}{dt d\omega_p}$, and ω_p represent the Hawking GUP-deformed temperature, emission energy, and photon frequency, respectively. We incorporated formulas to find the shadow radius and its spherically four-dimensional symmetrical metric. The shadow radius can be determined by a BH through the modification of the metric with a quintessence matter parameter. This generally implies a shadow deviation compared to the standard Schwarzschild BH. The shadow radius varies with the quintessence matter value, frequently evolving to reflect non-magnetized plasma closest to the horizon. This theoretical framework thus enables an analytical treatment of light propagation and shadow formation in quintessence matter in spacetime. The Hamiltonian expression is defined [109] as

$$H = \frac{1}{2} (g^{ik} j_i j_k + \omega_p^2(r)) \\ = \frac{1}{2} \left(-\frac{\mathbf{v}_t^2}{F_{tt}(r)} + G_{rr}(r) \mathbf{v}_r^2 + \frac{\mathbf{v}_\phi^2}{r^2} + \omega_p^2(r) \right). \quad (45)$$

The equations of motion for photons can be obtained by deriving the Hamiltonian (Eq. (42)) for a two-fluid source from Maxwell's equations. The conserved quantities $-\mathbf{v}_t = E$ and $\mathbf{v}_\phi = F_{tt}(r)$, which correspond to the photon energy and angular momentum, respectively, where \mathbf{v}_r represents the radial momentum given by

$$\dot{\mathbf{v}}_r = -\frac{\partial H}{\partial r} = \frac{1}{2} \left(-\frac{\mathbf{v}_t^2 F'_{tt}(r)}{F_{tt}^2(r)} + \mathbf{v}_r^2 G'_{rr}(r) - \frac{d}{dr} \frac{\mathbf{v}_\phi^2}{r^2} - \frac{d}{dr} \omega_p^2(r) \right). \quad (46)$$

For photons, we set $H = 0$ as

$$0 = -\frac{\mathbf{v}_t^2}{F_{tt}(r)} + \mathbf{v}_r^2 G_{rr}(r) + \frac{\mathbf{v}_\phi^2}{r^2} + \omega_p^2(r). \quad (47)$$

\mathbf{v}_t and \mathbf{v}_ϕ are constants of motion, and we can write $\omega_0 = -\mathbf{v}_t$. This relation allows us to express the photon frequency $\omega(r)$ measured by a static observer as a function of r :

$$\omega(r) = \frac{\omega_0}{\sqrt{F_{tt}(r)}}. \quad (48)$$

The orbit equation can be obtained as

$$\frac{dr}{d\phi} = \frac{G_{rr}(r) r^2 \mathbf{v}_r}{\mathbf{v}_\phi}. \quad (49)$$

Substituting \mathbf{v}_r into Eq. (44) gives

$$\frac{dr}{d\phi} = \pm r \sqrt{G_{rr}(r)} \sqrt{\frac{\omega_0^2 S^2(r)}{\mathbf{v}_\phi^2} - 1}. \quad (50)$$

For the frequency ω_0 measured by a static observer, the function $S(r)$ is defined as

$$S^2(r) = \frac{r^2}{F_{tt}(r)} \left(1 - F_{tt}(r) \frac{\omega_p^2(r)}{\omega_0^2} \right). \quad (51)$$

which leads to the general photon–sphere condition

$$2 - \frac{6M}{r_p} - 3(1 + \omega_q) \frac{C_q}{r_p^{1+3\omega_q}} \\ = \left(1 - \frac{2M}{r_p} - \frac{C_q}{r_p^{1+3\omega_q}} \right)^2 \left[\frac{2\omega_p^2(r_p)}{\omega_0^2} + \frac{2r_p}{\omega_0^2} \omega_p(r_p) \omega'_p(r_p) \right]. \quad (52)$$

The photon orbit equation illustrates the effects of quintessence (ω_q) matter and plasma on the photon sphere radius r_p . The photon sphere partially extends in comparison with the standard GR value for $\omega_q = 0$ (dust) or $1/3$ (radiation), which leads to a slightly larger shadow. In the cases of $\omega_q = -0.5$ (quintessence dark matter) and $\omega_q = -1$ (cosmological constant), the photon sphere is pulled inward by the modest reduction r_p caused by the negative pressure. For every scenario, homogeneous plasma ($\omega_p = \text{constant}$) adds a slight outward shift, but this effect is negligible in comparison with powerful gravitational influences. The observed shadows are yet compatible with conventional GR assumptions because these changes are generally minor and fall within the existing EHT observational uncertainties. This framework illustrates conceivable effects of various cosmic fluids on photon orbits near supermassive BHs.

Homogeneous plasma case $\omega'_p = 0$:

In a uniform plasma case in which the plasma frequency is steady in the BH in quintessence matter,

$$2 - \frac{6M}{r_p} - 3(1 + w_q) \frac{C_q}{r_p^{1+3w_q}} = 2 \left(1 - \frac{2M}{r_p} - \frac{C_q}{r_p^{1+3w_q}} \right)^2 \frac{\omega_p^2}{\omega_0^2}. \quad (53)$$

The interaction with the BH solution in quintessence matter affects the circular light orbit.

Vacuum limit case $\omega_p = 0$:

$$2 - \frac{6M}{r_p} - 3(1 + w_q) \frac{C_q}{r_p^{1+3w_q}} = 0. \quad (54)$$

This study evaluates and distinguishes between the homogeneous and vacuum limits of plasma surrounding BHs in quintessence matter interactions, focusing on their circular light orbits.

Given that X denotes the turning point of the trajectory, the condition $\left. \frac{dr}{d\phi} \right|_X = 0$ must hold. This associates X with the motion constant $\frac{v_\phi}{\omega_0}$ as

$$S^2(X) = \frac{v_\phi^2}{\omega_0^2}. \quad (55)$$

For a stationary observer at position r_0 , the light rays with angular radius β relative to the radial direction are given as

$$\cot\beta = \pm \frac{1}{\sqrt{G_{rr}(r)}} \frac{dr}{d\phi} \Big|_{r=r_0}. \quad (56)$$

Using Eq. (52), the orbit equation (Eq. (47)) can be rewritten as

$$\frac{dr}{d\phi} = \pm r \sqrt{G_{rr}(r)} \sqrt{\frac{S^2(r)}{S^2(X)} - 1}. \quad (57)$$

For the shadow radius ($R \approx \sin^2\beta$), we obtain

$$R = \frac{S^2(X)}{S^2(r_0)}. \quad (58)$$

The shadow radius (R) is defined by rays that asymptotically approach a circular photon orbit of radius r_{ph} . Hence, the angular shadow radius is obtained by taking $X \rightarrow r_{\text{ph}}$ in Eq. (55), giving

$$R = \frac{S^2(r_{\text{ph}})}{S^2(r_0)}. \quad (59)$$

In regions where the plasma density is sufficiently small around the observer, Eq. (48) simplifies to

$$S^2(r_0) = \frac{r_0^2}{F(r_0)}. \quad (60)$$

The equation (Eq. (55)) for shadow radius (R) can be determined as

$$R = \frac{r_{\text{ph}}^2 \left(1 - \frac{2M}{r_0} - \frac{C_q}{r_0^{1+3w_q}} \right)}{r_0^2 \left(1 - \frac{2M}{r_{\text{ph}}} - \frac{C_q}{r_{\text{ph}}^{1+3w_q}} \right)} \left(1 - \frac{\omega_p^2(r_{\text{ph}}) \left(1 - \frac{2M}{r_{\text{ph}}} - \frac{C_q}{r_{\text{ph}}^{1+3w_q}} \right)}{\omega_0^2} \right). \quad (61)$$

The shadow radius depends on the BH mass M , density related parameter C_q , state parameter ω_q , plasma frequency ω_p , observer frequency ω_0 , and photon and observer radii ω_{ph} and r_0 , respectively. It is worth mentioning here that we can recover the shadow of the Schwarzschild BH by setting $C_q = 0 = \omega_q$ and $r_{\text{ph}} = 3M$ in the given form:

$$R = \frac{27 M^2 (1 - 2M/r_0)}{r_0^2}. \quad (62)$$

In Fig. 5(i), the plot shows the dependence of the shadow radius R on photon radius r_{ph} for various values of the state parameter ω_q with respect to the other parameters being constant. It is clear that for all ω_q , the shadow R does increase with r_{ph} , and the black curve represents Schwarzschild case (Schw) used as a reference curve. However, for the curve with $\omega_q = -1$, the cosmological constant yields shadow radii R larger than in all other cases, again reaching the strongest lensing and thus the largest apparent shadow. As ω_q transitions from negative to positive values, the shadow radius R continues to decrease. This suggests that the effect of quintessence-like dark energy may weaken the BH's surrounding gravitational field, thereby reducing the optical shadow. This suggests that the region of photon capture does decrease with captured R .

In Fig. 5(ii), the plot shows how the shadow radius R is affected by the ratio of the parameters of the plasma frequency equation. The shadow radius R increases nonlinearly with r_{ph} for the ranges examined, though R generally increases with the plasma frequency ratio ω_p^2/ω_0^2 . The shadow for the $\omega_p^2/\omega_0^2 = 0.9$ curve is the largest, and the shadows become smaller for lower ratios. This indicates that the optical size of the BH shadow increases in denser plasma environments due to photon refraction and dispersion. This demonstrates that plasma environments should be incorporated into the equations in practical astrophysics in the observation of BH shadows.

We can formulate a new expression for emission energy through the combination of Eqs. (40) and (41) as follows:

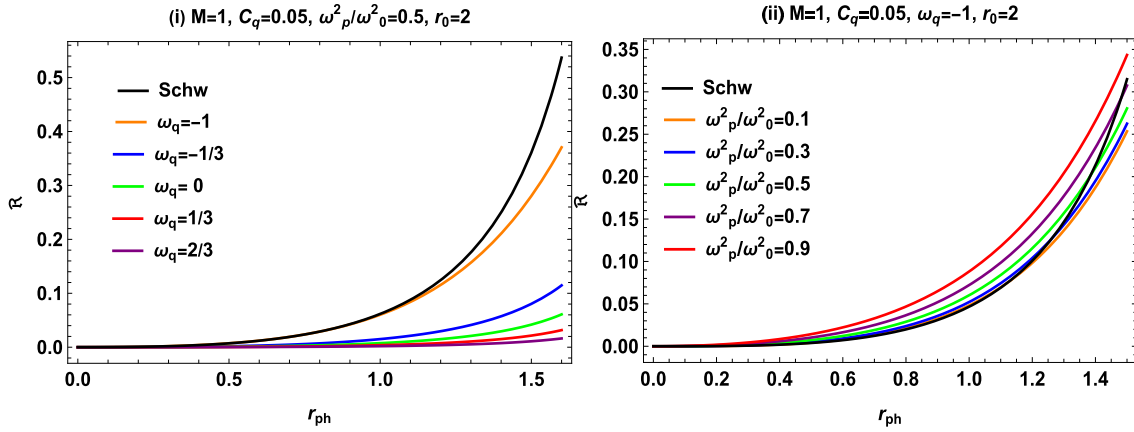


Fig. 5. (color online) Shadow radius R versus photon radius r_{ph} for varying values of state parameter ω_q and plasma frequency ratio ω_p^2/ω_0^2 .

$$E = \frac{2\pi^3 \omega_p^3 R^2}{\frac{\omega_p}{T'_H} - 1}. \quad (63)$$

We derived the emission energy in Eq. (60) for the quintessence matter geometry parameter of the BH function. This corresponds to a particle propagating under the action of a non-magnetized plasma and quantum gravity of a BH in quintessence matter. We also estimated the corresponding particle content at infinity of a boson field propagating in the BH spacetime by first considering the vacuum state before the collapse. A number of significant characteristics of the released energy E are apparent from Table 3. First, raising the quintessence normalisation parameter C_q causes E to fall monotonously, which indicates that the Hawking radiation emission is lowered by a stronger surrounding dark energy field. Second, the released energy rises as the equation-of-state parameter w_q becomes less negative for unchanged C_q , indicating that the radiation action is strengthened by weaker quintessence interactions. Additionally, the effective Hawking temperature T'_H is greatly decreased by the GUP correction parameter δ , leading to a severe suppression of E as δ increases. This action demonstrates that BH evapora-

tion is inhibited by quantum gravity considerations. Finally, the released energy is further reduced by the plasma frequency term $\omega_p^2(r_{\text{ph}})$. In the limit $\omega_p^2(r_{\text{ph}}) \rightarrow \omega_0^2$, photon propagation near the photon sphere is more limited as $\omega_p^2(r_{\text{ph}})$ increases, resulting in a significant fall in E and disappearing emission. Overall, the typical radiation spectrum is greatly altered by the combined impacts of quintessence, GUP corrections, and plasma context.

In Fig. 6(i), initially, the energy emission rate increases with the frequency of the emitted photons, reaches a peak value, and then sharply declines, confirming a peak emission value within the specified range. As ω_q increases from -1 to positive values, both the peak emission value and total emission rate decrease, indicating that even more negative values of ω_q enhance the emission. This is because negative (dark energy-like) states with close to zero ω_q values strengthen the emission from the BH due to the change in the curvature of the BH surroundings, horizon temperature, and BH emission rate.

In Fig. 6(ii), the emission within a BH is governed by the same principles, as the emission profile also possesses a spoke structure. However, the peak height of the

Table 3. E according to variations of model parameters.

Parameters	Variations	E	Physical interpretation
C_q	Increase	Decrease	Stronger quintessence suppresses radiation
C_q	Decrease	Increase	Weaker dark energy enhances emission
w_q	Increase (less negative)	Increase	Reduced repulsive effect of quintessence
w_q	Decrease (more negative)	Decrease	Stronger dark energy domination
δ	Increase	Decrease	GUP corrections lower T'_H
δ	Zero	Maximum	Classical Hawking limit recovered
$\omega_p^2(r_{\text{ph}})$	Increase	Decrease	Plasma suppresses photon propagation
$\omega_p^2(r_{\text{ph}})$	Approaches ω_0^2	Approaches zero	Cutoff of emitted radiation

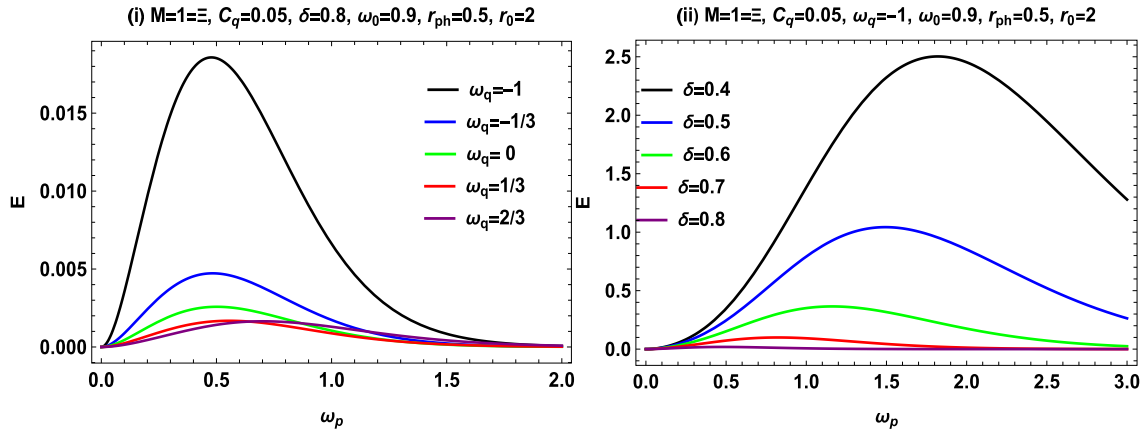


Fig. 6. (color online) Energy emission rate E as a function of photon frequency ω_p with fixed $M = 1 = \Xi$, $C_q = 0.05$, $\omega_0 = 0.9$, $r_{ph} = 0.5$, and $r_0 = 2$ for varying values of state parameter ω_q with fixed $\delta = 0.8$ and varying values of GUP parameter δ with fixed $\omega_q = -1$.

emission profile decreases systematically with the value of the parameter δ , as lower δ values correspond to the emission of stronger BH energy. This is an indication that the quantum gravity effect is in the construction of a lower δ value, which in turn increases the emission of lower energy photons. The peak emission value for a BH decreases with increasing δ , which further signifies that stronger GUP effects result in a greater decrease of a BH's effective temperature and radiation emission, confirming quantum effects in the process of moderating the Hawking emission decrease.

In short, the GUP thermodynamic corrections of physical importance originate from the potential to help explain quintessence-deformed (dark matter) background BH dynamics with the basic principles of quantum physics. This suggests a possible resolution to the data paradox and also enhances the study of the basic features of gravity and spacetime on the quantum level.

VI. CONCLUSIONS

Parikh and Wilczek proposed a quantum tunneling mechanism to derive Hawking radiation. We assume that, in a BH in quintessence matter, a particle-antiparticle pair forms closest to the horizon. The associated vector fields of particles can be classified into outgoing forms that radiate the BH horizon with quintessence matter and ingoing forms that are inside it. The incoming boson particles are located on the horizon. Furthermore, certain outgoing forms are related to quantum tunneling occurrence, with the barrier of the horizon to a certain point when the boson outgoing particles from the BH in quintessence matter. If a particle with positive energy leaves this dimension, it may cross the horizon in relation to BH radiation. Both such a particle and its antiparticle can exist indefinitely. We calculated the WKB approximation for tunneling-modified probability, considering the logically prohibited trajectory. By applying a Hamilton-Jacobi semi-

classical approach to compare the tunneling modified probability with the Boltzmann factor, we were able to detect the Hawking temperature. It is important to note that we have ignored the impacts of the radiation from particle back-reaction and self-gravity. We have adapted the Lagrangian GUP-deformed expression to explain the action of the spin-1 particle. We determined the realistic temperatures and tunneling probability of particles based on a BH in quintessence matter. The corrected tunneling depends not only on the characteristics of the BH in quintessence matter but also on the angular momentum-energy and mass of the escaped particles. The spacetime structure and quantum modifications determine the modified Hawking temperature for a BH in quintessence matter. At zeroth order in the semi-classical mechanism, the original Hawking correction terms are comparable. To maintain the GUP, the first-order corrective term must be less than the preceding term.

In realistic astrophysical situations, especially those affected by dark matter, this relationship is significantly modified. Dark matter's gravitational influence alters the spacetime geometry around the BH, affects its thermodynamic equilibrium, and drives entropy changes due to statistical and quantum corrections. Furthermore, the creation and destruction of specific particle pairs near the horizon's limits allow positive-energy particles to escape the BH in quintessence matter through tunneling in the region where Hawking radiation occurs. The BH in quintessence matter evaporates due to this tunneling mechanism in the form of Hawking radiation. It has been demonstrated that, for a far-off observer, its absorption cross-section reaches the BH shadow with quintessence matter. To further investigate the basic dynamics of BH spacetime in the framework of quintessence matter, the more powerful gravity model can be used to examine the physical characteristics of the BH incorporating the GUP parameter.

APPENDIX A

We generate the equation system presented, disreg-

arding higher orders in the Lagrangian GUP-deformed expression (Eq. (26)) and considering only the term h in the WKB approximation for the 1st order. We get

$$\begin{aligned} G(r) & \left[c_1(\partial_0 H_0)(\partial_1 H_0) + \delta c_1(\partial_0 H_0)^3(\partial_1 H_0) - c_0(\partial_1 H_0)^2 - \delta c_0(\partial_1 H_0)^4 \right] \\ & + \frac{1}{r^2} \left[c_2(\partial_0 H_0)(\partial_2 H_0) + \delta c_2(\partial_0 H_0)^3(\partial_2 H_0) - c_0(\partial_2 H_0)^2 - \delta c_0(\partial_2 H_0)^4 \right] \\ & + \frac{1}{r^2 \sin^2 \theta} \left[c_3(\partial_0 H_0)(\partial_3 H_0) + \delta c_3(\partial_0 H_0)^3(\partial_3 H_0) + c_0(\partial_3 H_0)^2 + \delta c_0(\partial_3 H_0)^4 \right] - c_0 m^2 = 0, \end{aligned} \quad (A1)$$

$$\begin{aligned} -\frac{1}{F(r)} & \left[c_0(\partial_0 H_0)(\partial_1 H_0) + \delta c_0(\partial_0 H_0)(\partial_1 H_0)^3 - c_1(\partial_0 H_0)^2 - \delta c_1(\partial_0 H_0)^4 \right] \\ & + \frac{1}{r^2} \left[c_2(\partial_1 H_0)(\partial_2 H_0) + \delta c_2(\partial_1 H_0)^3(\partial_2 H_0) - c_1(\partial_2 H_0)^2 - \delta c_1(\partial_2 H_0)^4 \right] \\ & + \frac{1}{r^2 \sin^2 \theta} \left[c_3(\partial_1 H_0)(\partial_3 H_0) + \delta c_3(\partial_1 H_0)^3(\partial_3 H_0) - c_1(\partial_3 H_0)^2 - \delta c_1(\partial_3 H_0)^4 \right] - c_1 m^2 = 0, \end{aligned} \quad (A2)$$

$$\begin{aligned} \frac{1}{F(r)} & \left[c_0(\partial_0 H_0)(\partial_2 H_0) + \delta c_0(\partial_0 H_0)(\partial_2 H_0)^3 - c_2(\partial_0 H_0)^2 - \delta c_2(\partial_0 H_0)^4 \right] \\ & - G(r) \left[c_2(\partial_1 H_0)^2 + \delta c_2(\partial_1 H_0)^4 - c_1(\partial_1 H_0)(\partial_2 H_0) - \delta c_1(\partial_1 H_0)(\partial_2 H_0)^3 \right] \\ & + \frac{1}{r^2 \sin^2 \theta} \left[c_3(\partial_2 H_0)(\partial_3 H_0) + \delta c_3(\partial_2 H_0)^3(\partial_3 H_0) - c_2(\partial_3 H_0)^2 - \delta c_2(\partial_3 H_0)^4 \right] + m^2 c_2 = 0, \end{aligned} \quad (A3)$$

$$\begin{aligned} \frac{1}{F(r)} & \left[c_0(\partial_0 H_0)(\partial_3 H_0) + \delta c_0(\partial_0 H_0)(\partial_3 H_0)^3 - c_3(\partial_0 H_0)^2 - \delta c_3(\partial_0 H_0)^4 \right] \\ & + G(r) \left[c_3(\partial_1 H_0)^2 + \delta c_3(\partial_1 H_0)^4 - c_1(\partial_3 H_0)(\partial_1 H_0) - \delta c_1(\partial_1 H_0)(\partial_3 H_0)^3 \right] \\ & + \frac{1}{r^2} \left[c_3(\partial_2 H_0)^2 + \delta c_3(\partial_2 H_0)^4 - c_2(\partial_2 H_0)(\partial_3 H_0) - \delta c_3(\partial_2 H_0)(\partial_3 H_0)^3 \right] - m^2 c_3 = 0. \end{aligned} \quad (A4)$$

APPENDIX B

Considering a 4×4 matrix, we employ Eq. (61):

$$K(c_0, c_1, c_2, c_3)^T = 0. \quad (B1)$$

$$\begin{aligned} K_{00} & = G(r)(W_r^2 + \delta W_r^4) \\ & \quad - \frac{1}{r^2}(J^2 + \delta J^4) + \frac{1}{r^2 \sin^2 \theta}(W_\theta^3 + \delta W_\theta^4) - m^2, \\ K_{01} & = -G(r)(E + \delta E^3)W_r, \\ K_{02} & = -\frac{1}{r^2}(E + \delta E)J, \\ K_{03} & = -\frac{W_\theta}{r^2 \sin^2 \theta}(E + \delta E^3), \end{aligned}$$

The created matrix is not trivial. Its elements are as fol-

lows:

$$\begin{aligned}
K_{10} &= \frac{EW_r + \delta EW_r^3}{F(r)}, \\
K_{11} &= \frac{E^2 + \delta E^4}{F(r)} - \frac{J^2 - \delta J^4}{r^2} \\
&\quad - \frac{1}{r^2 \sin^2 \theta} (W_\theta^2 - \delta W_\theta^4) - m^2, \\
K_{12} &= \frac{1}{r^2} (W_r + \delta W_r^3) J, \\
K_{13} &= \frac{1}{r^2 \sin^2 \theta} (W_r + \delta W_r^3) W_\theta, \\
K_{20} &= -\frac{1}{F(r)} (EJ + \delta EJ^3) \\
K_{21} &= G(r) (W_r J + \delta J^3 W_r), \\
K_{22} &= \frac{1}{F(r)} (E^2 + \delta E^4) \\
&\quad - G(r) (W_r^2 + \delta W_r^4) - \frac{1}{r^2 \sin^2 \theta} (W_\theta^2 + \delta W_\theta^4) - m^2 \\
K_{23} &= \frac{1}{r^2 \sin^2 \theta} (J + \delta J^3) W_\theta, \\
K_{30} &= -\frac{1}{F(r)} (EW_\theta + \delta EW_\theta^3), \\
K_{31} &= -G(r) (W_\theta + \delta W_\theta^3) W_r, \\
K_{32} &= -\frac{1}{r^2} (W_\theta + \delta W_\theta^3) J, \\
K_{33} &= -\frac{1}{F(r)} (E^2 + \delta E^4) + G(r) (W_r^2 + \delta W_r^4) \\
&\quad - \frac{1}{r^2} (J^2 + \delta J^4) - m^2, \tag{B2}
\end{aligned}$$

with $E = \partial_t H_0$, $W_r = \partial_r H_0$, $W_\theta = \partial_\theta H_0$, and $J = \partial_\phi H_0$.

References

- [1] A. Einstein, *Annalen Phys.* **354**, 769 (1916)
- [2] A. Einstein, *The Collected Papers of Albert Einstein* (Princeton: Princeton University Press, 1997), p. 496.
- [3] V. P. Frolov and A. Zelnikov, *Introduction to Black Hole Physics* (Oxford: Oxford University Press, 2011), p. 506.
- [4] S. W. Hawking, *A brief history of time* (New York: Bantam Books, 1998).
- [5] S. W. Hawking, *Nature* **248**, 30 (1974)
- [6] S. W. Hawking, *Comm. Math. Phys.* **43**, 199 (1975)
- [7] X. Q. Li, *Phys. Lett. B* **763**, 80 (2016)
- [8] S. W. Hawking, *Phys. Rev. D* **13**, 191 (1976)
- [9] M. Sharif and W. Javed, *Eur. Phys. J. C* **72**, 1997 (2012)
- [10] R. Ali, R. Babar, M. Asgher *et al.*, *Chin. J. Phys.* **86**, 269 (2023)
- [11] W. Javed, R. Babar, and A. Övgün, *Mod. Phys. Lett. A* **34**, 1950057 (2019)
- [12] W. Javed, R. Ali, R. Babar *et al.*, *Eur. Phys. J. Plus* **134**, 511 (2019)
- [13] W. Javed, R. Ali, R. Babar *et al.*, *Chin. Phys. C* **44**, 015104 (2020)
- [14] V. E. Akhmedova, T. Pilling, A. de Gill *et al.*, *Theor. Math. Phys.* **163**, 774 (2010)
- [15] T. Zhu, J. R. Ren, and D. Singleton, *Int. J. Mod. Phys. D* **19**, 159 (2010)
- [16] M. Hossain Ali, *Class. Quantum Grav.* **24**, 5849 (2007)
- [17] R. Babar, Z. Akhtar, M. Asgher *et al.*, *Indian J. Phys.* **97**, 3155 (2023)
- [18] W. Javed, R. Ali, and G. Abbas, *Can. J. Phys.* **97**, 176 (2018)
- [19] M. Hossain Ali, *Gen. Relat. Gravit.* **36**, 1171 (2004)
- [20] E. T. Akhmedov, V. Akhmedova, and D. Singleton, *Phys. Lett. B* **642**, 124 (2006)
- [21] X. M. Kuang, J. Saavedra, and A. Övgün, *Eur. Phys. J. C*

- [22] M. K. Parikh and F. Wilczek, *Phys. Rev. Lett.* **85**, 5042 (2000)
- [23] M. Angheben, M. Nadalini, L. Vanzo *et al.*, *JHEP* **05**, 014 (2005)
- [24] P. Kraus and F. Wilczek, *Nucl. Phys. B* **433**, 403 (1995)
- [25] P. Kraus and F. Wilczek, *Nucl. Phys. B* **437**, 231 (1995)
- [26] M. K. Parikh, *Phys. Lett. B* **546**, 189 (2002)
- [27] R. Ali, R. Babar, M. Asgher *et al.*, *Int. J. Mod. Phys. A* **37**, 2250108 (2022)
- [28] R. Ali, X. Tiecheng, H. Aounallah *et al.*, *Indian J. Phys.* **98**, 3741 (2024)
- [29] M. Banados, C. Teitelboim, and J. Zanelli, *Phys. Rev. Lett.* **69**, 1849 (1992)
- [30] R. Ali, R. Babar, M. Asgher *et al.*, *Int. J. Geom. Methods Mod. Phys.* **19**, 2250017 (2022)
- [31] R. Ali, X. Tiecheng, and R. Babar, *Nucl. Phys. B* **1008**, 116710 (2024)
- [32] J. de Oliveira and R. D. B. Fontana, *Phys. Rev. D* **98**, 044005 (2018)
- [33] S. I. Kruglov, *Mod. Phys. Lett. A* **29**, 1450203 (2014)
- [34] R. Ali, R. Babar, M. Asgher *et al.*, *Ann. Phys.* **432**, 168572 (2021)
- [35] R. Kerner and R. B. Mann, *Class. Quant. Grav.* **25**, 095014 (2008)
- [36] R. Ali, K. Bamba, M. Asgher *et al.*, *Int. J. Mod. Phys. D* **30**, 2150002 (2021)
- [37] R. Ali, K. Bamba, S. A. A. Shah *et al.*, *Int. J. Mod. Phys. D* **31**, 2250069 (2022)
- [38] X. Calmet, R. Casadio, and F. Kuipers, *Phys. Rev. D* **100**, 086010 (2019)
- [39] A. O. Barvinsky and G. A. Vilkovisky, *Phys. Lett. B* **131**, 313 (1983)
- [40] A. O. Barvinsky and G. A. Vilkovisky, *Phys. Rep.* **119**, 1 (1985)
- [41] A. O. Barvinsky and G. A. Vilkovisky, *Nucl. Phys. B* **282**, 163 (1987)
- [42] A. O. Barvinsky and G. A. Vilkovisky, *Nucl. Phys. B* **333**, 471 (1990)
- [43] I. L. Buchbinder, S. D. Odintsov, and I. L. Shapiro, *Effective Action in Quantum Gravity*, (Bristol: CRC Press, 1992), p. 424.
- [44] J. F. Donoghue, *Phys. Rev. D* **50**, 3874 (1994)
- [45] X. Calmet, *Phys. Lett. B* **787**, 36 (2018)
- [46] G. Gecim and Y. Sucu, *Eur. Phys. J. Plus* **132**, 105 (2017)
- [47] G. Gecim and Y. Sucu, *Adv. High Energy Phys.* **2018**, 7031767 (2018)
- [48] G. Gecim and Y. Sucu, *Phys. Lett. B* **773**, 391 (2017)
- [49] M. Dernek, C. Tekincay, G. Gecim, *et al.*, *Eur. Phys. J. Plus* **138**, 369 (2023)
- [50] C. Tekincay, G. Gecim, and Y. Sucu, *EPL* **135**, 31003 (2021)
- [51] D. Gangopadhyay and G. Manna, *EPL* **100**, 49001 (2012)
- [52] G. Manna and B. Majumder, *Eur. Phys. J. C* **79**, 553 (2019)
- [53] B. Chatterjee, A. Ghosh, and P. Mitra, *Phys. Lett. B* **661**, 307 (2008)
- [54] P. Mitra, *Phys. Lett. B* **648**, 240 (2007)
- [55] K. H. Chae, A. V. Kravtsov, J. A. Frieman *et al.*, *J. Cosmol. Astropart.* **11**, 004 (2012)
- [56] H. N. Luu, P. Mocz, M. Vogelsberger *et al.*, *Phys. Rev. D* **111**, L121302 (2025)
- [57] A. Burkert, *ApJ* **904**, 161 (2020)
- [58] J. A. Schewtschenko, R. J. Wilkinson, C. M. Baugh *et al.*, *Mon. Not. Roy. Astron. Soc.* **449**, 3587 (2015)
- [59] S. Carlip, *Class. Quant. Grav.* **17**, 4175 (2000)
- [60] J. Makela and P. Repo, arXiv: gr-qc/9812075
- [61] A. Chatterjee and P. Majumdar, arXiv: gr-qc/0303030
- [62] G. Gour and A. J. M. Medved, *Class. Quant. Grav.* **20**, 3307 (2003)
- [63] J. W. York, *Phys. Rev. D* **33**, 2092 (1986)
- [64] M. M. Akbar and S. Das, *Class. Quant. Grav.* **21**, 1383 (2004)
- [65] F. J. Wang, Y. X. Gui, and C. R. Ma, *Phys. Lett. B* **660**, 144 (2008)
- [66] R. Ali, R. Babar and M. Asgher, *Annalen der Physik* **2200074**, 12 (2022)
- [67] R. Ali, R. Babar, and P. K. Sahoo, *Phys. Dark Univ.* **35**, 100948 (2022)
- [68] R. Ali and M. Asgher, *New Astron.* **93**, 101759 (2022)
- [69] A. Övgün and K. Jusufi, *Eur. Phys. J. Plus* **131**, 177 (2016)
- [70] I. Sakalli, A. Övgün, and K. Jusufi, *Astrophys Space Sci.* **361**, 330 (2016)
- [71] R. Ali, X. Tiecheng, and R. Babar, *Gen. Relativ. Gravit.* **56**, 13 (2024)
- [72] S. Kanzi and I. Sakalli, *Nucl. Phys. B* **946**, 114703 (2019)
- [73] F. Ahmed, A. Al-Badawi, I. Sakalli *et al.*, *Nucl. Phys. B* **1011**, 116806 (2025)
- [74] E. Aydiner, E. Sucu, and I. Sakalli, *Phys. Dark Univ.* **50**, 102164 (2025)
- [75] I. Sakalli and S. Kanzi, *Ann. Physics* **439**, 168803 (2022)
- [76] H. Gursel and I. Sakalli, *Can. J. Phys.* **94**, 2 (2016)
- [77] I. Sakalli and A. Övgün, *Gen. Rel. Grav.* **48**, 1 (2016)
- [78] E. Sucu and I. Sakalli, *Phys. Dark Univ.* **49**, 102051 (2025)
- [79] F. Ahmed, A. Al-Badawi, and I. Sakalli, *Eur. Phys. J. C* **85**, 984 (2025)
- [80] X. Q. Li, G. R. Chen, *Phys. Lett. B* **751**, 34 (2015)
- [81] V. V. Kiselev, *Class. Quant. Grav.* **20**, 1187 (2003)
- [82] A. Belhaj, A. El Balali, W. El Hadri *et al.*, *Eur. Phys. J. Plus* **134**, 422 (2019)
- [83] S. Cheng and J. Jing, *Class. Quantum Grav.* **22**, 4651 (2005)
- [84] K. Meng, J. Zhao, M. Deng *et al.*, *Phys. Lett. B* **868**, 139630 (2025)
- [85] K. Konishi, G. Paffuti, and P. Provero, *Phys. Lett. B* **234**, 276 (1990)
- [86] M. Maggiore, *Phys. Lett. B* **319**, 83 (1993)
- [87] L. J. Garay, *Int. J. Mod. Phys. A* **10**, 145 (1995)
- [88] G. Amelino-Camelia, *Int. J. Mod. Phys. D* **11**, 1643 (2002)
- [89] A. Kempf, G. Mangano, and R. B. Mann, *Phys. Rev. D* **52**, 1108 (1995)
- [90] F. Scardigli, *Phys. Lett. B* **452**, 39 (1999)
- [91] F. Scardigli and R. Casadio, *Class. Quant. Grav.* **20**, 3915 (2003)
- [92] S. Hossenfelder, M. Bleicher, S. Hofmann *et al.*, *Phys. Lett. B* **575**, 85 (2003)
- [93] O. Nairz, M. Arndt, and A. Zeilinger *et al.*, *Phys. Rev. A* **65**, 032109 (2002)
- [94] I. Pikovski, M. R. Vanner, M. Aspelmeyer *et al.*, *Nature Phys.* **8**, 393 (2012)
- [95] M. Kober, *Phys. Rev. D* **82**, 085017 (2010)
- [96] K. Nozari and S. H. Mehdipour, *Europhys. Lett.* **84**, 20008 (2008)
- [97] R. Ali, R. Babar, H. Aounallah *et al.*, *Int. J. Geom. Methods Mod. Phys.* **21**, 2450149 (2024)

- [98] K. Umetsu, *Int. J. Mod. Phys. A* **25**, 4123 (2010)
- [99] K. Umetsu, *Phys. Lett. B* **692**, 61 (2010)
- [100] A. Sen, *JHEP* **04**, 156 (2012)
- [101] R. Banerjee and B. R. Majhi, *Phys. Lett. B* **662**, 62 (2018)
- [102] R. Banerjee and B. R. Majhi, *JHEP* **2008**, 095 (2008)
- [103] R. Banerjee, B. R. Majhi, and S. Samanta, *Phys. Rev. D* **77**, 124035 (2008)
- [104] R. Ali, X. Tiecheng, and R. Babar, *Phys. Dark Univ.* **48**, 101868 (2025)
- [105] R. Ali, X. Tiecheng, and R. Babar, *Fortschr. Phys.* **73**, e70017 (2025)
- [106] U. Papnoi, F. Atamurotov, S. G. Ghosh *et al.*, *Phys. Rev. D* **90**, 024073 (2014)
- [107] R. Ali, X. Tiecheng, M. Awais *et al.*, *Chinese J. Phys.* **94**, 416 (2025)
- [108] S. W. Wei and Y. X. Liu, *J. Cosmol. Astropart.* **11**, 063 (2013)
- [109] V. Perlick, O. Y. Tsupko, and G. S. Bisnovatyi-Kogan, *Phys. Rev. D* **92**, 104031 (2015)